

## Observation of Resonant Photon Drag in a Two-Dimensional Electron Gas

A. D. Wieck, H. Sigg, and K. Ploog

*Max-Planck-Institut für Festkörperforschung, Heisenbergstrasse 1, D-7000 Stuttgart 80, Federal Republic of Germany*

(Received 29 November 1989)

We observe a photon-drag voltage along the optical path of photons propagating in the plane of an unbiased 2D electron gas in GaAs quantum wells. This voltage is induced by momentum transfer from 10- $\mu\text{m}$ -wavelength photons to the electrons, resonantly matched in their intersubband energy to the photons by appropriate choice of the 8.2-nm well width. The voltage is reversed when the propagation direction of the photons is reversed. Moreover, the sign of the voltage also changes by sweeping the photon energy through the intersubband resonance condition, in agreement with current theory.

PACS numbers: 72.40.+w, 73.50.Pz, 78.20.Jq

The photon-drag effect (PDE) is the light-induced particle drift due to the momentum transfer from photons to the particles. These particles may be atoms in a gas<sup>1,2</sup> or electrons in a solid. In the latter case the PDE induces a voltage drop along the way of the photons in the solid, which can be detected via electric probes at different sites along the optical path. Since the PDE response time is correlated to the very short momentum relaxation time of the charge carriers, various scattering mechanisms can be sensed with this effect and there are potential applications as rapid photon detectors. Many investigations have been performed on heavily *p*-doped Ge, where the photons induce transitions between heavy- and light-hole states, leading to the momentum transfer from photons to holes and thus to the photon-drag voltage.<sup>3-7</sup> However, in this case only a small fraction of the carriers is in resonant interaction with photons of a given energy due to the high nonparallelism of the valence energy bands in Ge, thus reducing the efficiency of the PDE. This situation changes drastically if the energy bands of the ground and the excited states are parallel, which occurs in Landau bands in a magnetic field (cyclotron resonance or spin resonance) and in the subbands of a 2D electron gas (2DEG). Whereas theory predicts PDE in all three cases,<sup>8-11</sup> up to now and to our knowledge, only the cyclotron-resonance PDE<sup>12</sup> has been observed experimentally.<sup>13</sup> In a recent paper, Luryi<sup>10</sup> predicted the existence of the PDE in a 2DEG, which should be enhanced by the parallel subbands and different momentum relaxation times in the two lowest subbands. The aim of this Letter is to investigate this system experimentally and, as to be seen below, to give the first experimental evidence for this enhanced PDE in a 2DEG.

The key point for the successful experiment is the precise sample fabrication, i.e., the intentional matching of the quantum well width (and thus the intersubband energy) with the spectral range of the photon source. In order to get easily achievable and stable infrared power densities into the sample, we choose as photon source a CO<sub>2</sub> laser. As the center wavelength of the CO<sub>2</sub> modes

is 10  $\mu\text{m}$ , the intersubband-resonance energy has to match the corresponding energy of 124 meV. The appropriate quantum well width evaluated by interpolation of the known intersubband-resonance energies<sup>14,15</sup> is 8.2 nm. This width, corresponding to 29 GaAs monolayers, must be attained precisely since a deviation of only one monolayer changes the intersubband energy by 4.5%,<sup>15</sup> which is at the band limits of the CO<sub>2</sub> laser. We therefore grow the sample by molecular-beam epitaxy: On 300- $\mu\text{m}$ -thick semi-insulating GaAs, we deposit 200-nm GaAs, followed by 300-nm Al<sub>0.35</sub>Ga<sub>0.65</sub>As. After the Si-doped ( $10^{18}\text{-cm}^{-3}$ ) 5-nm Al<sub>0.35</sub>Ga<sub>0.65</sub>As layer, we grow a 15-nm Al<sub>0.35</sub>Ga<sub>0.65</sub>As spacer (\*) and the 8.2-nm-thick GaAs quantum well (\*), followed in a symmetrical manner by the 15-nm Al<sub>0.35</sub>Ga<sub>0.65</sub>As spacer (\*), the 5-nm Si-doped Al<sub>0.35</sub>Ga<sub>0.65</sub>As, 300-nm Al<sub>0.35</sub>Ga<sub>0.65</sub>As, and 5-nm GaAs. This single-quantum well is denoted sample *A*, whereas sample *B* comprises a 30-quantum well structure, in which the sequence (\*) plus 10-nm Si-doped ( $10^{18}\text{-cm}^{-3}$ ) Al<sub>0.35</sub>Ga<sub>0.65</sub>As is repeated 29 times before growing the 30th quantum well similar to the single well of sample *A*. Alloyed AuGe contacts to the mesa-etch-defined area of  $3\times 6\text{ mm}^2$  [Fig. 1(b)] allow Hall measurements as well as the observation of the photon-drag voltage. Table I shows carrier concentration *n*, mobility  $\mu$ , and the corresponding momentum scattering time in the lowest subband  $\tau_1 = m\mu/e$ , where *m* is the effective mass of  $0.07m_e$ . The sample is mounted in good thermal contact to a liquid-He-cooled cold-finger cryostat with optical access via two windows. Similar to previous intersubband-resonance (ISR) experiments on GaAs<sup>16</sup> we use a quasistrip-line technique to couple the radiation into the sample: Wedging and polishing both the entrance and the exit facet for the beam at Brewster's angle  $\phi_B = 74^\circ$  with respect to the normal of the 2DEG [Fig. 1(b)], the radiation inside the sample is *p* polarized (components of  $\mathbf{E} \perp 2\text{DEG}$ ) which is the only mode to excite ISR. A good parallelism between the two facet planes is necessary to get the transmitted light in parallel with the direction of the incident light. The radiation passing in the sample is reflected approximately 10 times

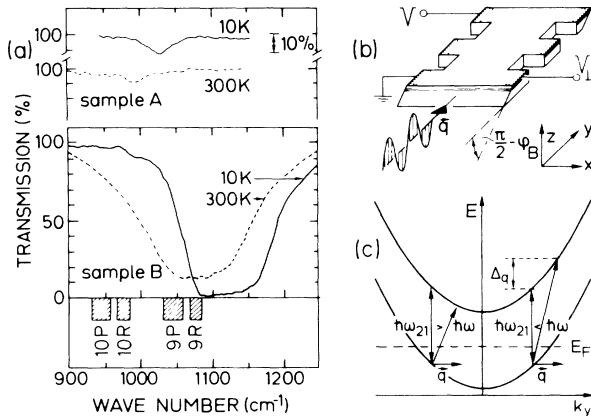


FIG. 1. (a) Intersubband resonances measured in transmittance of single (sample *A*) and 30-period (sample *B*) 8.2-nm-thick GaAs-Al<sub>0.35</sub>Ga<sub>0.65</sub>As quantum wells at temperatures  $T=10$  and 300 K, respectively. The CO<sub>2</sub> laser bands used in the following figures are indicated on the wave-number scale at the bottom. (b) Schematic sketch of the sample geometry with the incident light wave vector  $\mathbf{q}$  in the plane of the 2DEG.  $V$  denotes the electric potential measured along the optical path in the  $y$  direction, whereas  $V_{\perp}$  is measured perpendicularly to  $\mathbf{q}$ . Shaded areas indicate contact metallizations. (c) Nonvertical transitions of photons of wave vector  $\mathbf{q}$  and energy  $\hbar\omega$  between the lowest and the first excited parabolic subband with the  $\mathbf{k}=0$  ISR energy  $\hbar\omega_{21}$ . Note that for  $\hbar\omega < \hbar\omega_{21}$ , only transitions with negative  $k_y$  are possible, whereas for  $\hbar\omega > \hbar\omega_{21}$  only transitions with positive  $k_y$  are excited. For clarity,  $\mathbf{q}$  has been enlarged by a factor of about  $10^3$  in this figure.

at the frontside and the backside of the sample, traversing the 2DEG 20 times. Care has been taken to not illuminate the contact regions by placing an aperture of  $0.3 \times 3 \text{ mm}^2$  in front of the sample and to focus the radiation onto the sample such that the transmission is the strongest. The transmitted intensity is detected by a liquid-N<sub>2</sub>-cooled InSb detector or a piezoelectric detector, respectively.

In order to estimate the ISR energy,<sup>17</sup> we first perform transmission experiments with a fast-scan Fourier-transform spectrometer. Spectra taken at room temperature and low temperature ( $T=10 \text{ K}$ ), normalized to the frequency response without sample, are shown in Fig. 1(a). Intersubband resonances are observed for both

TABLE I. Electron concentration  $n$ , mobility  $\mu$ , and scattering times  $\tau_1$  in the lowest and  $\tau_2$  in the first excited subband for sample *A*. While  $n$ ,  $\mu$ , and  $\tau_1$  are deduced from Hall measurements,  $\tau_2$  is measured via the width of the intersubband resonance (see text). The experimental accuracy for all values is 10%.

$T$ (K)	$n$ ( $10^{12} \text{ cm}^{-2}$ )	$\mu$ ( $\text{m}^2/\text{Vs}$ )	$\tau_1$ (ps)	$\tau_2$ (ps)
300	0.59	0.46	0.18	0.13
10	0.99	1.98	0.79	0.15

sample *A* and sample *B*. The increase of the resonance energy with decreasing temperature is a known feature of the ISR in quantum wells but not yet well understood theoretically.<sup>15</sup> In the single well (sample *A*) the ISR exhibits a peak height of 11% at  $T=10 \text{ K}$ . The full width at half maximum (FWHM)  $2\hbar\gamma$  is estimated to be 5.2 meV, where  $2\gamma=1/\tau_1+1/\tau_2$  with the momentum scattering time  $\tau_1$  in the lowest and  $\tau_2$  in the first excited subband, respectively.<sup>10,11</sup> As the energy of the excited subband is 3.6 times higher than the optical phonon energy,  $\tau_2$  is strongly limited by phonon emission and thus governs the width of the ISR. For this reason, the ISR does not become much broader in raising  $T$  to room temperature. In principle, nonparabolicity can also lead to a broadening of the ISR due to not completely parallel subbands. However, even a theoretically assumed mass difference of 10% between the two subbands only weakly broadens the ISR.<sup>15</sup> The scattering times  $\tau_2$  deduced from the FWHM are listed in Table I. They are significantly shorter than the corresponding  $\tau_1$  values, which is a necessary condition for the existence of the enhanced photon-drag effect.<sup>10,11</sup>

Intersubband resonances in the multiple quantum wells of sample *B* are much stronger than in the single-quantum well discussed before. The line shape becomes saturated and the transmission of the sample dramatically drops to zero in a frequency band wider than  $60 \text{ cm}^{-1}$ . We concentrate in this Letter on the spectra of the single-well sample, in which the total absorption is only of the order of 10% and the photon flux is thus distributed homogeneously over the whole sample length.

In Fig. 2 the photon-drag voltage and the corresponding laser power are shown for laser lines of the 10P band. By smoothly tilting the line-selecting grating of the laser by a motor system, we tune the laser over all possible lines, recording the intensity and drag voltage via standard lock-in techniques versus the tilt angle of the grating. Whereas the single laser lines represent distinct frequencies, the closely spaced line spectrum allows a quasi-frequency sweep.

The geometrical arrangement of the contacts and the direction of the incident light wave vector  $\mathbf{q}$  are sketched on the right-hand side of Fig. 2. In Fig. 2(b) the room-temperature drag voltage  $V$  is plotted for the 10P band. As the photon energy  $\hbar\omega$  is smaller than the ISR energy, only ISR transitions with negative  $k_y$  (i.e., electron wave vector  $\mathbf{k}$  antiparallel to  $\mathbf{q}$ ) are excited, inducing holes with negative  $k_y$  in the lowest subband and electrons with a smaller negative  $k_y$  in the first excited subband [see Fig. 1(c)]. Because  $\tau_2 < \tau_1$ , the excited electrons lose their direction more rapidly than the holes in the lowest subband. This leads to a net current of holes in the direction of  $-\mathbf{q}$ , the enhanced PDE.<sup>10,11</sup> The corresponding negative drag voltage  $V$  is exactly what we measure in Fig. 2(b). A crucial test for the nature of this observed voltage is its behavior in reversing the photon path by turning the sample. In this case, the

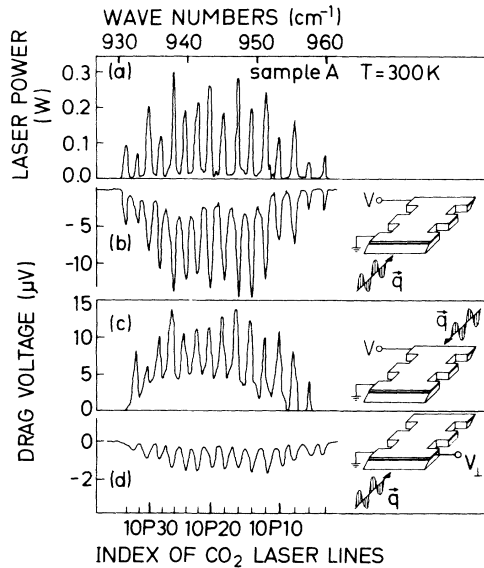


FIG. 2. (a) CO<sub>2</sub> laser power for different lines of the 10P band, representing a quasifrequency sweep. (b)–(d) Room-temperature photon-drag effect voltage vs frequency for  $\hbar\omega < \hbar\omega_{21}$  and different experimental setups as indicated on the right-hand-side insets. In reversing  $\mathbf{q}$ , the drag voltage is reversed. The transverse photon drag is about 1 order of magnitude smaller [(d)] than the longitudinal [(b) and (c)] one.

photon-drag voltage should only change its sign. Once again, this is exactly, what we observe [Fig. 2(c)].

This longitudinal drag voltage at room temperature is as high as 14  $\mu\text{V}$  for a laser power of 0.3 W. The transverse photon drag, measured with the potential probes located on a line perpendicular to  $\mathbf{q}$  [Fig. 2(d)], is about 10 times smaller than the longitudinal one. Theoretically, the transverse photon drag should be zero for symmetry reasons. In fact, the small voltages  $V_{\perp}$  recorded here vary from contact pair to contact pair even in their sign, indicating that residual transverse light modes exist in the crystal.

In Fig. 3, the photon-drag voltage measured at low temperatures in the configuration of Fig. 2(b) is plotted over the whole frequency range of the CO<sub>2</sub> laser. The striking feature of this plot is that the drag voltage changes its sign when the photon energy is raised above the ISR energy of 1027  $\text{cm}^{-1}$  measured in Fig. 1(a). Under this condition, only transitions with positive  $k_y$  are allowed [see Fig. 1(c)], leaving unoccupied states with  $k_y > 0$  in the lowest subband. They lead to a net hole current in the  $k_y$  direction, and thus to a positive drag voltage. The sign change of the drag voltage in the as-observed polarity is the specific signature of the resonantly enhanced photon-drag effect in a 2DEG.<sup>10,11</sup>

In Fig. 4, the drag current is normalized on the laser power and plotted versus frequency. We obtain this short-circuit drag current by dividing the measured open-loop drag voltage by the source impedance of the sample of about 1 k $\Omega$ . In addition, the transmission

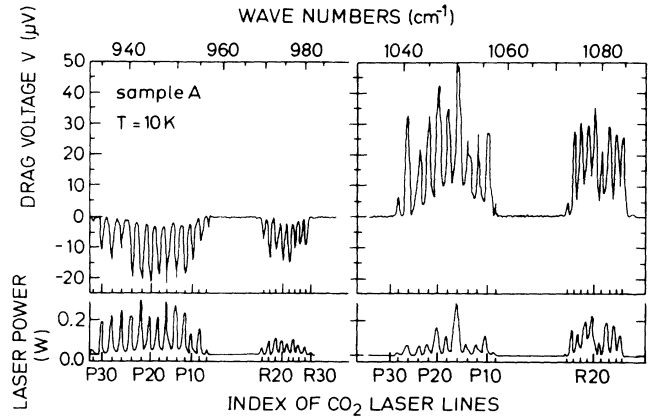


FIG. 3. Low-temperature photon-drag voltage (upper traces) and corresponding laser power (lower traces) for a wide spectrum of CO<sub>2</sub> laser lines. Increasing the photon energy from below to above the intersubband energy of 1027  $\text{cm}^{-1}$  [see Fig. 1(a)] changes the sign of the induced drag voltage from negative to positive.

change due to the intersubband excitation is shown on the same frequency scale. The resonant enhancement of the drag voltage in the vicinity of the ISR is evident. The slopes of the positive and negative branches suggest a singular point very close to the ISR energy, where the

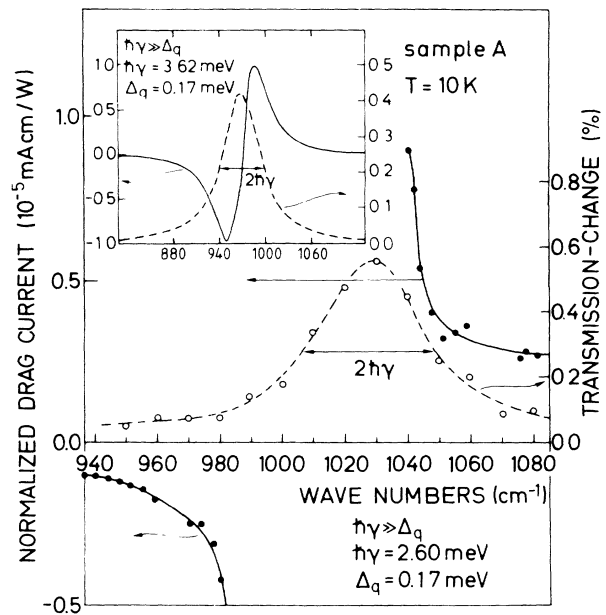


FIG. 4. Experimental intersubband-resonance transmission change per transversed quantum well from Fig. 1(a) (O) and photon-drag short-circuit current, normalized on the laser-power density and sample length (●), respectively. Lines are guides to the eye. Inset: Calculated spectra from Ref. 11, whose parameters are very close to the experimental ones as indicated in the figure. The axis scales of the inset refer to the lettering of the main figure.

PDE vanishes. The inset shows the theoretical prediction of the effect, which supposes almost the same parameters of  $n=10^{12} \text{ cm}^{-2}$  and the Doppler shift  $\Delta_q=0.17 \text{ meV}$ .<sup>11</sup> Both the ISR oscillator strength and the photon-drag current coincide within 30% with the observed values, which can be regarded as a satisfactory agreement.

On sample *B*, we observe only a negative drag voltage of the same height as in sample *A*, because the ISR lies just above the CO<sub>2</sub> laser mode range. This sample is well matched to 50- $\Omega$  impedances, and we can probe the speed of the PDE response via 100-ns rise-time pulses of the laser. The laser intensity evolution of the pulses is accurately reproduced in the photon-drag voltage, indicating that inherent time constants are much shorter than 100 ns. This observation confirms that thermal effects at the contacts or *phonon*-drag effects are not important in the measurements presented here, because their time constants are given by the sample dimensions divided by the sound velocity, which is of the order of several  $\mu\text{s}$ .

In conclusion, we present the first experimental evidence for a resonant photon-drag effect in a 2DEG, which is due to momentum transfer between photons and electrons. It leads to a voltage drop along the optical path in the sample, which offers the feasibility of very fast and simple radiation detectors. Since the effect depends strongly on the relaxation times in different subbands, the kinetics of various scattering mechanisms can be studied. The quantitative agreement between theory and experiment is surprisingly good and offers an understanding not only of the energy but also of the momentum transfer between photons and electrons in solids.

We gratefully acknowledge the skillful assistance with the Fourier spectrometer by W. König and financial support of the Bundesministerium für Forschung und Tech-

nologie of the Federal Republic of Germany.

<sup>1</sup>H. G. C. Werij, J. E. M. Haverkort, and J. P. Woerdman, *Phys. Rev. A* **33**, 3270 (1986).

<sup>2</sup>H. G. C. Werij, J. E. M. Haverkort, P. C. M. Planken, E. R. Eliel, J. P. Woerdman, S. N. Atutov, P. L. Chapovskii, and F. Kh. Gel'mukhanov, *Phys. Rev. Lett.* **58**, 2660 (1987).

<sup>3</sup>A. M. Danishevskii, A. A. Kastal'skii, S. M. Ryvkin, and I. D. Yaroshetskii, *Zh. Eksp. Teor. Fiz.* **58**, 544 (1970) [*Sov. Phys. JETP* **31**, 292 (1970)].

<sup>4</sup>A. F. Gibson, M. F. Kimmitt, and A. C. Walker, *Appl. Phys. Lett.* **17**, 75 (1970).

<sup>5</sup>T. Kamibayashi, S. Yonemochi, and T. Miyakawa, *Appl. Phys. Lett.* **22**, 119 (1973).

<sup>6</sup>P. J. Bishop, A. F. Gibson, and M. F. Kimmitt, *IEEE J. Quantum Electron.* **9**, 1007 (1973).

<sup>7</sup>G. A. F. Ali, S. Montasser, L. Zaki, S. M. Refaei, and L. El-Nadi, *Appl. Phys. A* **39**, 291 (1986).

<sup>8</sup>E. M. Skok and A. M. Shalagin, *Pis'ma Zh. Eksp. Teor. Fiz.* **32**, 201 (1980) [*JETP Lett.* **32**, 184 (1980)].

<sup>9</sup>A. M. Dykhne, V. A. Roslyakov, and A. N. Starostin, *Dokl. Akad. Nauk SSSR* **254**, 599 (1980) [*Sov. Phys. Dokl.* **25**, 741 (1980)].

<sup>10</sup>S. Luryi, *Phys. Rev. Lett.* **58**, 2263 (1987).

<sup>11</sup>A. A. Grinberg and S. Luryi, *Phys. Rev. B* **38**, 87 (1988).

<sup>12</sup>A. F. Kravchenko, A. M. Palkin, V. N. Sozinov, and O. A. Shegai, *Pis'ma Zh. Eksp. Teor. Fiz.* **38**, 328 (1983) [*JETP Lett.* **38**, 393 (1983)].

<sup>13</sup>J. P. Woerdman, *Phys. Rev. Lett.* **59**, 1624 (1987).

<sup>14</sup>L. C. West and S. J. Eglash, *Appl. Phys. Lett.* **46**, 1156 (1985).

<sup>15</sup>P. von Allmen, M. Berz, G. Petrocelli, F. K. Reinhart, and G. Harbeke, *Semicond. Sci. Technol.* **3**, 1211 (1988).

<sup>16</sup>A. D. Wieck, K. Bollweg, U. Merkt, G. Weimann, and W. Schlapp, *Phys. Rev. B* **38**, 10158 (1988).

<sup>17</sup>In this paper, we discuss the depolarization-shifted ISR energy (Ref. 16), neglecting to a good approximation the  $\mathbf{k}$  dependence of the depolarization shift.

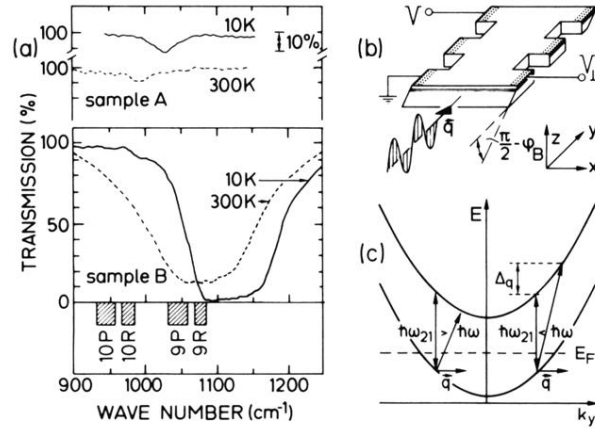


FIG. 1. (a) Intersubband resonances measured in transmittance of single (sample *A*) and 30-period (sample *B*) 8.2-nm-thick GaAs-Al<sub>0.35</sub>Ga<sub>0.65</sub>As quantum wells at temperatures  $T=10$  and 300 K, respectively. The CO<sub>2</sub> laser bands used in the following figures are indicated on the wave-number scale at the bottom. (b) Schematical sketch of the sample geometry with the incident light wave vector  $\mathbf{q}$  in the plane of the 2DEG.  $V$  denotes the electric potential measured along the optical path in the  $y$  direction, whereas  $V_{\perp}$  is measured perpendicularly to  $\mathbf{q}$ . Shaded areas indicate contact metallizations. (c) Nonvertical transitions of photons of wave vector  $\mathbf{q}$  and energy  $\hbar\omega$  between the lowest and the first excited parabolic subband with the  $\mathbf{k}=0$  ISR energy  $\hbar\omega_{21}$ . Note that for  $\hbar\omega < \hbar\omega_{21}$ , only transitions with negative  $k_y$  are possible, whereas for  $\hbar\omega > \hbar\omega_{21}$  only transitions with positive  $k_y$  are excited. For clarity,  $\mathbf{q}$  has been enlarged by a factor of about  $10^3$  in this figure.